Vol. 11(7), pp. 129-142, July-September 2019
DOI: 10.5897/IJWREE2019.0837
Article Number: 628E5C461761
ISSN: 2141-6613

http://www.academicjournals.org/IJWREE

ACADEMIC JOURNALS
expand your knowledge

International Journal of Water Resources and Environmental Engineering

Full Length Research Paper

Enhancing the adsorption of Pb(II) and Fe(II) in the reactor by the thermally treated alluvial clay from Far North Cameroon

Adjia Zangué H.[1,2*], Nga B.[2], Kamga R.[2], Villiéras F.[1] and Ebio Nko'o G.[3]

[1]Laboratoire Interdisciplinaire des Environnements Continentaux (LIEC) UMR 7360 CNRS-Université de Lorraine 15 Avenue du Charmois, 54500 Vandœuvre-lès-Nancy, France
[2]National School of Agro-Industrial Sciences (ENSAI) University of Ngaoundere B.P. 455 Adamaoua, Cameroon.
[3]Department of Chemistry, Faculty of Science (FS) University of Ngaoundere B.P. 454 Ngaoundere, Cameroon.

Received 28 January, 2019; Accepted 25 April, 2019

The objective of this work was to investigate the influence of the thermal treatment of alluvial clay on the ad-sorption capacity of Pb(II) and Fe(II) to reduce clogging during adsorption phenomenon. The chemical, X- ray diffraction (XRD), Fourier transform infrared spectroscopy (FTIR), scanning electron microscope (SEM) and transmission electron microscopy (TEM) analysis of the alluvial clays reveal that the main mineral present is smectite, kaolinite and quartz. Cation exchange capacity (CEC) and specific surface area of the raw clay fraction are 62 meq/100 g and 104 m2/g respectively. The mains oxydes of alluvial clay fraction<50µm are SiO2, Al2O3 and Fe2O3.The adsorbent used in this work is the alluvial clay, that after splitting has been thermally treated at 300°C and 600°C, the natural clay properties does not completely disappear until 300°C and 600°C. This study shows that the losses are about 3% for the heat treatment at 300°C (A300) and 5% for the heat treatment at 600°C (A600) after fractionation of Alluvial clays. The adsorption equilibrium is reached in five minutes, whatever the pH, temperature and the molar ratio of the solution. The pH is increased the removal increases as seen from plots of 2, 4 and 6 which gave removals as high as 92.15µmol/g and 100.6 µmol/g to Pb(II) and 92.68 µmol/g and 110.5 µmol/g to Fe(II) respectively. The temperature is decreased the removal increases as seen from plots of 50°C, 40°C and 30°C which gave removals as high as 99.8 µmol/g and 100.3 µmol/g to Pb(II) and 98.9 µmol/g and 100.3 µmol/g to Fe(II) respectively. While, the adsorption capacity was increased as decreasing the temperature. So, it is be recognized that adsorption mechanism should be physical adsorption. The adsorption process of Pb(II) and Fe(II) are best described by the second-order equation. However, the adsorption isotherms could be well fitted by the Freundlich equation, proves the surface heterogeneity of thermally treated Alluvial Clay.

Key words: Adsorption, agitated reactor, thermally treated alluvial clay, Cameroon.

INTRODUCTION

The pollution of water and/or soil, accidentally and/or voluntarily, by some chemicals of industrial origin (phenols, hydrocarbons, dyes ...) or agricultural (pesticides, fertilizers ...) constitutes a source of environmental degradation and is currently of particular interest internationally (Bouras, 2003; Demin et al., 2013).

Recent industrial revolution in central Africa as

Cameroon has enormously increased the industrial wastewater production which is highly contaminated with various types of heavy metals. Heavy metal contamination exists in waste effluents of different factories such as metal plating, mining operations, tanneries, ceramic painting, manufacturing paints, catalysts, alloy industries, galvanizing iron, polymer stabilizer, storage batteries manufacturing, pesticides, wood preservation, pigments factories and families cloths painting (Basso et al., 2002; Sundar et al., 2010; Arwidsson et al., 2010; Berthelot et al., 2008; Cao et al., 2008; Moon et al., 2010; Chrastný et al., 2010). Heavy metals have been acknowledged as potential health and environmentally hazardous materials. Many studies have shown that these metals are toxic even at low concentrations. The presence of these toxic metals can in turn, cause accumulative poisoning, destroy liver, cancer and brain damage when found above the tolerance level (Arif et al., 2015; Geier et al., 2015; Carneiro et al., 2014; Chen et al., 2012; Ilyin et al., 2010; Bridges and Zalups, 2010; Ilyin et al., 2002, 2003; CACAR, 2003; Carretero et al., 2002; Chang, 1977). Additionally, another problem in our study area is the presence of iron on the soil and this iron migrated in water process. Presently, many techniques such as chemical precipitation, extraction, reverse osmosis and adsorption are being used for the removal of heavy metals from wastewater. Adsorption technique is an economical process especially using low cost adsorbents. Many investigators have evaluated natural clay and the date pits as low-cost adsorbents due to their adsorption properties for heavy metals including cobalt, lead, cadmium, zinc and chromium ions (Ahmad et al., 2011, 2018; Sameeh et al., 2016; Abdullah et al., 2017; Ahmad et al., 2018). In contrast, there are very few studies on the mineralogy and use of clays from vertisol of the northern region of Cameroun. None of the above studies are dealing with alluvial clay of the far north region of Cameroon. In fact, Adjia et al. (2014) discovered new adsorbent, alluvial clay as alternative solution to resolve waste water problem.

Lead and iron are considered dangerous micropollutants. In fact, Lead is the heavy metal and Iron is presented on the littoral soil, affects processing water, and decreases by this fact the rentability of the industries in this economical area of Cameroon.

The toxicity affected by these heavy metals is considered high even in trace amounts (IARC, 1992; Curren et al., 2015). Given the variable quality of the contaminated water and the harmful effects of pollution, this metal as micropollutant is reduced by adsorption on the alluvial clay. Using alluvial clays as adsorbents is of interest in the removal of pollutants. This is justified by the importance of the surface developed by this material, by the presence of negative charges on the surface, by the possibility of exchange of the cations and by a wide availability in nature (Adjia et al., 2014).

However, many studies showed that, during the adsorption phenomenon in the reactor we have the clogging problem (Vishal et al., 2013). The aim of this work is to investigate the influence of heat treatment of a Alluvial clay on its adsorption capacity of Pb (II) and Fe (II) in the reactor.

MATERIALS AND METHODS

Alluvial clay materials

Study area and sampling

The soil samples were taken in a dry river bed situated between the towns of Maroua and Kaele in the far-north region of Cameroun (Picture 1). The system coordinates of this area is 10°02.883N and 014°23.084E. The climate is tropical-dry, characterized by 7- 8 months of dry season and 4 - 5 months of wet season. The mean annual rainfall and temperature in the area is 800 mm and 28.5°C, respectively. During the wet season, the rivers (locally call Mayo) contain running water while in the dry season there is almost no water. The soil depth during the sampling is 99 cm (**Adjia et al., 2013, 2014**).These soil samples were packaged in plastic packaging.

The soil fraction <50 µm (A50)

In this study, we focused on the size fraction <50 µm. The soil aggregate is pulverized in a mortar and then homogenized. About 1 kg of this sample is soaked in 2 L of distilled water for 4 h. This mixture is homogenized by subjecting to wet sieving with a 50-µm mesh sieve. The water is then removed by drying at 105°C in an oven for 24 h. The solid obtained was treated with 5% hydrogen peroxide solution to eliminate organic matter. The dried fraction is sprayed in an Agathe mortar; the powder obtained is weighed and stored in a sealed jar; and the clay fraction <2 µm (A02) was extracted by sedimentation. However, especially in this work, the resulting mixture was then sieved over 50-µm (A50) mesh sieve.

Mineralogy and physicochemical properties

X-ray diffraction (XRD): The X-ray diffraction (XRD) data were obtained using a D8 Bruker diffractometer with $CoK\alpha_1$ radiation (λ= 1.789 Å). Spectra were recorded on oriented and unoriented samples. The detection limit for a given crystalline phase is estimated at around 1% in mass. Ethylene glycol and heat treatments (550°C) were used to provide additional information essential for the identification of clay minerals.

Fourier Transform Infra Red (FTIR): Infrared spectra were recorded using an IFS 55 Bruker Fourier transform IR spectrometer equipped with an MCT detector (6000 to 600 cm^{-1}) cooled at 77K and in diffused reflectance (Harrick attachment) mode. The amount. of clay was 70 mg dispersed in 370 mg KBr

*Corresponding author E-mail: hzangue42@gmail.com.

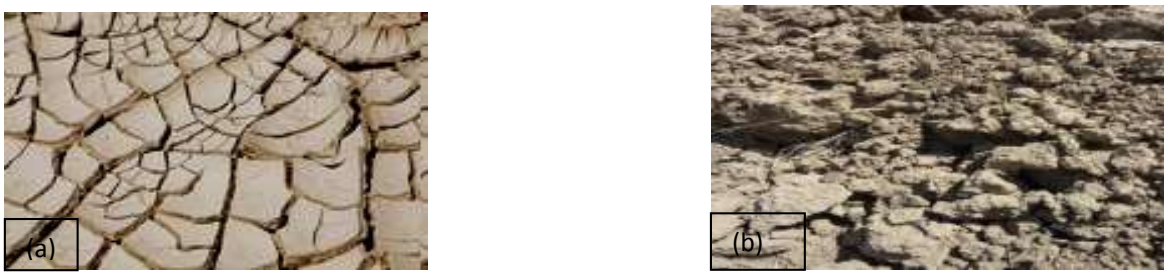

View A

View B (10°02883N et 014°23.084E)

Picture 1. View A: a) Mayo dried up; b) place of sampling. View B: a) sampling method.

Scanning and transmission electron microscopy: TEM observations were conducted with a Philips CM20 microscope equipped with an EDS detector. Secondary and backscattering SEM observations were carried out on a Hitachi 2500 LB SE microscope equipped with a Kevex Delta EDS spectrometer. SEM was used to assist in the identification of individual accessory minerals incorporated in the clay samples by comparing their morphological characteristics with their elemental compositions.

Chemical analyses: These were performed on the two clay fractions. The major elements were determined by inductively coupled plasma atomic emission spectroscopy (ICP-AES), whereas trace elements and rare earths elements were determined by inductively coupled plasma mass spectrometry (ICP-MS).

Cation exchange capacities (CEC): These were measured using cobaltihexamine [$Co(NH_3)_6Cl_3$] as exchangeable ions. The amount of cobaltihexamine fixed by the solid phase was determined from concentration measurements using UV-vis spectroscopy. The displaced cations were determined by atomic absorption spectrometry (Perkin-Elmer 1100B). The equilibrium pHs of clay suspensions were determined using a standard LPH 330 T electrode.

Textural properties: Nitrogen adsorption-desorption isotherms at 77K were recorded on a step-by-step automatic home-built set up. Pressures were measured using 0-1000 Pa and 0-100.000 Pa Baratron-type pressure sensors provided by Edwards. The nitrogen saturation pressure was recorded in situ using an independent 0-100.000 Pa Baratron-type pressure sensor provided by Edwards. Prior to adsorption, the samples were outgassed overnight at 120°C and under residual pressure of 0.01 Pa. Nitrogen N55 (purity > 99.9995%) used for experiments was provided by alphagaz (France). Specific surface areas (SSA) were determined from adsorption data by applying the Brunauer-Emmet-Teller (BET) equation and using 16.3Å^2 for the cross sectional area of nitrogen. In the present study, error in the determination of the SSA was estimated as +/- 1 m^2/g. Micropores volumes and non-microporous surface areas were obtained using the t-plot method proposed by De Boer et al. (1996). Pore size distributions were calculated on the desorption branch using the Barrett-Joyner-Halenda method, assuming slit-shaped pores.

Heat treatment

The treatment is carried out using a muffle furnace. It consists in weighing the crucible empty, then putting 159.94 g of alluvial clay fraction in the crucible, weighed, and then the sample was introduced into the oven at different temperatures from room temperature (25±1°C) to the temperature set for 40 min at 300°C and 70 min at 600°C. Finally, it was allowed to cool and the samples weighed again.

Experimental procedures

Lead salts ($Pb(NO_3)_2$) and Mohr salt ($Fe(NH_4)_2(SO_4)_2,6H_2O$) are used for the preparation solutions, using waste water conditions. All experiments were carried out at pH 7.0 (except when the effect of pH was studied). The pH of each solution was adjusted to the desired value by addition of dilute HCl or NaOH solutions.

Preparation of solutions and Adsorption phenomenon

The initial lead solution at 4826µmol/L was prepared by dissolving 0.81g of lead nitrate salt ($PbNO_3)_2$ hydrated in 500ml of distilled water. The resulting solution was stored in a one-liter flask. This solution has been diluted to provide solutions of desired concentrations during adsorption.

The initial solution of 17851 µmol/L Iron was prepared by dissolving 3.5 g of hydrated Mohr salt ($Fe(SO_4)_2(NH_4)_2(SO_4)_2,6H_2O$) in 500 ml of distilled water. The resulting solution was stored in a one-liter flask.

For the adsorption experiments, 25 ml of lead nitrate solution (289.6 µmol/L) and Mohr salt at a concentration of 1071.4 µmol/L are introduced into a 50-ml series of Erlenmeyer flasks. The whole solution is kept at ambient temperature (25 ±1°C) and stirred with a water bath at a constant speed of 120 rpm. Subsequently, 0.25 g of alluvial clay of each sample is introduced into each Erlenmeyer flask. These are then stirred at approximately 60 rpm at constant temperature for a period of one hour. At each time interval, the contents of the Erlenmeyer flask are filtered on Whatman N°1 filter paper. The optical density read at the visible spectrophotometer is converted into concentration and the amount of lead and iron adsorbed per unit mass of alluvial clay is given by the relation

$$q_{e=(C_o-C_e)}\frac{V}{m_{adsorbant}}\ (mg/g) \quad (1)$$

Where, qe is the amount of the metal adsorbed; C_0 is the initial concentration of the solution (µmol/L); C the concentration of the solution at time t in (µmol/L); m is the mass of alluvial clay used in (g) and V is the volume of the solution in (mL). The wavelength of 539 nm was used for Pb(II) analysis and 510 nm for Fe(II) analysis.

Effect of pH: The work is carried out in a pH range of between 2 to 6 in steps of 2 to observe the difference of the amounts adsorbed in an acidic.

Effect of temperature: To measure the influence of temperature, we will have three temperatures between 30 and 50°C, initial concentration, adsorbent and normal pH. Temperature has two major effects on the adsorption process.

Modeling of adsorption kinetics: Adsorption kinetics were studied using the pseudo-first-order, pseudo-second-order and intraparticular diffusion equations.

i) Kinetic model of pseudo-first order: The velocity equation of the pseudo-first-order kinetic model is given by the relation:

$$\log(q_e - q_t) = logq_e - \frac{k_1 t}{2{,}303} \quad (2)$$

Where q_e and q_t are respectively the relative amounts adsorbed at the adsorption equilibrium at time t, and k_1 (min^{-1}) is the pseudo-first order rate constant. Representing the log (q_e – q_t) = f(t) function, we obtain a straight line of slope - $\frac{k}{2.303}$ and an intercept of log qe (Harouna et al., 2015).

ii) Kinetic model of pseudo-second order: The pseudo-second-order kinetic model can be represented in the following form:

$$\frac{t}{q_t} = \frac{1}{k_2 q_e^2} + \frac{t}{q_e} \quad (3)$$

Where q_e and q_t are respectively the relative quantities adsorbed at equilibrium and at time t, k_2 is the pseudo-second-order rate constant (Harouna et al., 2015).

iii) Kinetic model of intra particle diffusion: The intraparticular diffusion model can be represented by the equation:

$$q_t = k_{int}\sqrt{t} + C \quad (4)$$

Where q_t is the relative amount of adsorbed Lead and Iron at time t, k_{int} is the intraparticular diffusion constant and C is a constant **(Reddy et al., 2010)**. The regression of the function $q_t = f(\sqrt{t})$, makes it possible to obtain a line of slope k_{int} and ordinate at the origin C.

Modeling adsorption isotherms: The adsorption capacity was determined using the isotherms of Langmuir and Freundlich.

i) Langmuir model: The theory proposed by Langmuir is based on a homogeneous distribution of the adsorption sites. The Langmuir isotherm can be represented by the equation:

$$q_e = \frac{aK_L C_e}{1+K_L C_e} \quad (5)$$

Where C_e is the residual relative amount at the adsorption equilibrium, q_e, the relative amount of the adsorbed Lead and Iron per gram of adsorbent has the adsorbed amount for the monolayer and K_L the equilibrium adsorption constant (Domga et al., 2015).

ii) Freundlich model: The simple and empirical model of Freundlich is the second most commonly used model. It is considered that it applies to many cases, especially in the case of an adsorbent with a heterogeneous adsorption surface (energetically different adsorption sites).

$$q_e = K_F C_e^{\frac{1}{n}} \quad (6)$$

The linear expression of the Freundlich equation is obtained by taking the logarithm of the equation:

$$lnq_e = lnK_F + \frac{1}{n} lnC_e \quad (7)$$

Where K_F and *n* are the constants respectively reflecting the measurement of the adsorption capacity and the adsorbent-adsorbate affinity (Harouna et al., 2015).

RESULTS AND DISSCUSION

Mineralogy and physicochemical properties

X-ray diffraction

XRD patterns of alluvial clay samples show that it consists predominantly in smectite, kaolinite and quartz, with accessory minerals such as anatase, microcline, albite and rutile (Figure 1a). Results of the ethylene glycol test on oriented clay fraction showed the characteristic displacement of the basal peak of smectite from 15.2 to 18.3 Å (Figure 1b). The usual displacement of the smectite from 15.2 to 10.1Å on heating at 550°C is also observed. All the vertisol profiles in this area showed a similar mineralogical composition; however, Adjia et al. (2013, 2014) found that most of the smectite minerals of the vertisol soil of this zone are mixtures of montmorillonite and beidellite. The spectra of the A50

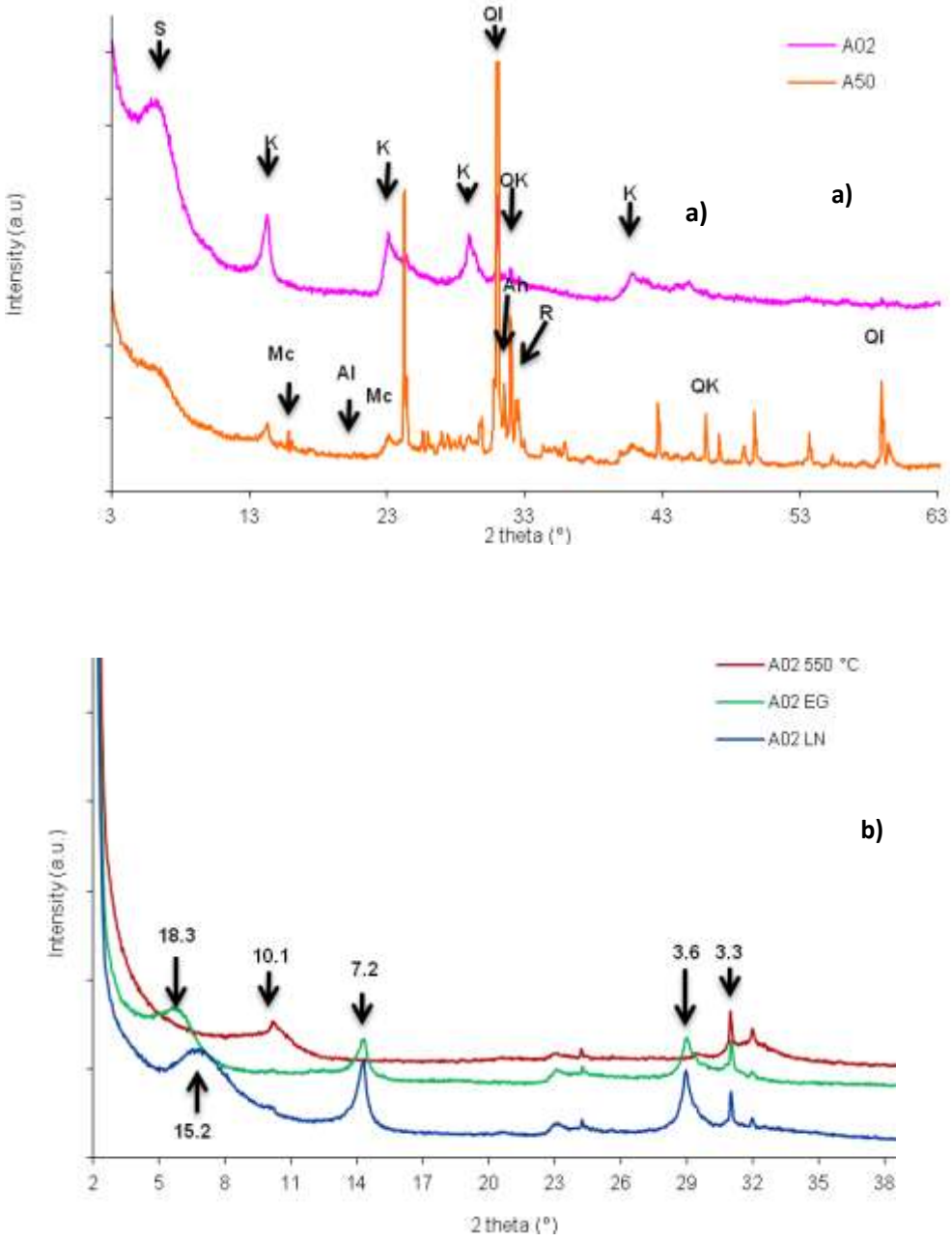

Figure 1. a) X-ray diffraction patterns of a) natural (A02, A50), **b)** oriented preparation of clay fraction (A02 LN), (A02 EG), (A02 550°C). Basal spacings on fig.1b are given in Å. Legend: (S: smectite ; K : kaolinite ; Mc : microcline ; Al : albite ; Q : quartz ; An : anatase ; R : rutile; I: illite)

fraction show a well-defined peak of quartz indicating a high amount of quartz in this sample. On the contrary, the clay fraction only presents very few amount of quartz.

Infrared spectroscopy

The infrared spectra of the two clays fractions are presented in Figure 2. The two spectra have almost the same feature. IR analysis confirms that smectite and kaolinite are the main mineral present in our clay samples. The broad band at 3390 cm^{-1} is usually attributed to the adsorbed water at the interlayer of smectite clays. The band at 1612 cm^{-1} is also attributed to smectite interlayer water. The band at 3698 cm^{-1} is assigned to the OH stretching vibration of kaolinite, whereas the band at 3620 cm^{-1} is characteristic of the OH stretching of kaolinite and of AlAlOH or AlMgOH groups

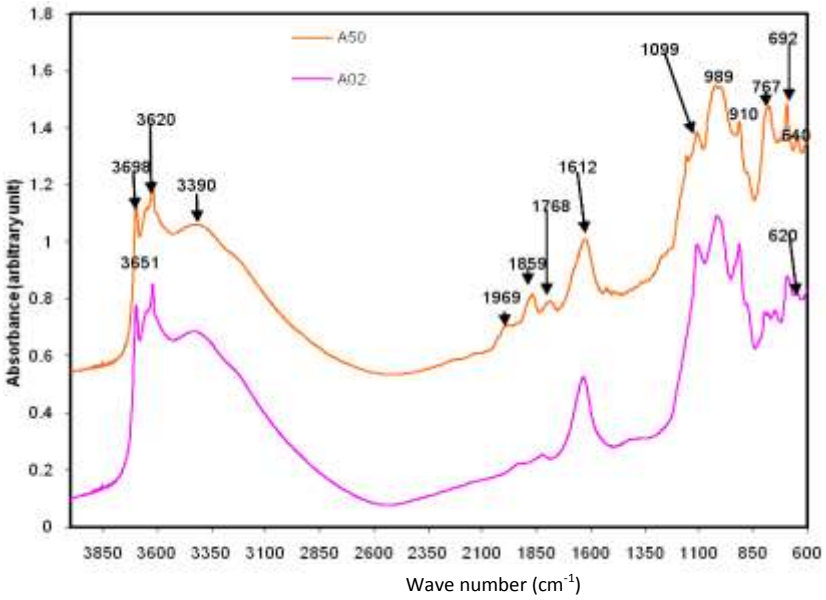

Figure 2. Infrared spectrum of the Alluvial Clay A02 and A50.

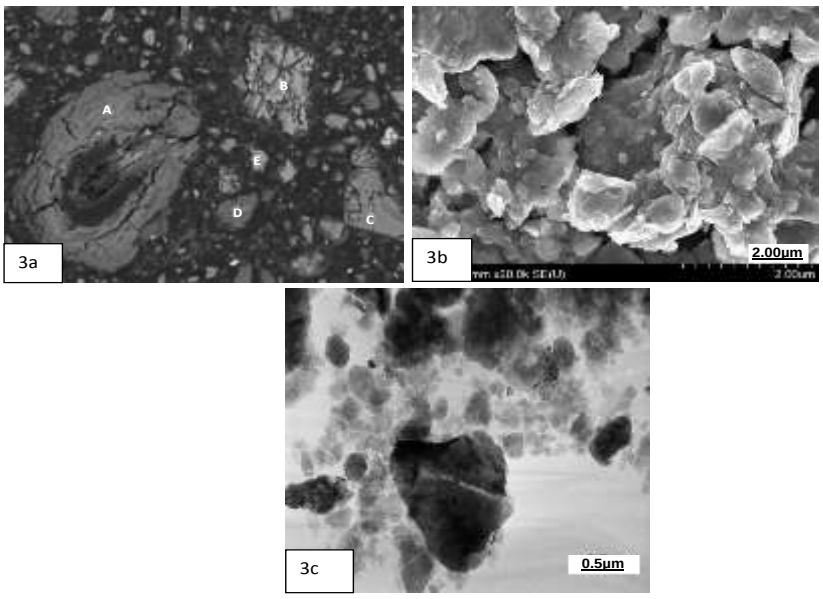

Figure 3. Scanning electron photomicrograph (SEM) and TEM micrograph of alluvial clayey fraction , showing typical texture.**3a)** SEM A50 (polished slide of clay embedted in resins); **3b)** SEM A50 (powder) ; **3c)** TEM A02. Minerals identification is derived from EDX analyses.

of smectite. In addition, IR analysis shows the absence of calcium or magnesium carbonates and of organic matter in the studied samples.

Scanning and transmission electron microscopy

SEM observation on a polish slide of A50 fraction shows large aggregates and small particles dispersed over the entire matrix (Figure 3a). SEM with EDX analysis of the aggregates reveal the presence of smectite [A]: (Si/Al≈0.60), of microcline [B]: (Si/Al≈2.8 and 3), of quartz [C]: (Al=0), of interstratified [D]: (Si/Al≈1.6) and of kaolinite [E]: (Si/Al≈2). Those minerals have currently been identified from XRD and IR analyses. The SEM images of A50 powder shows the usual cluster of rose

Table 1. Chemical analysis of major elements on a sandy fraction <50 µm (A50) and clayey fraction< 2 µm (A02).

Sample (%)	SiO_2	Al_2O_3	Fe_2O_3	MnO	MgO	CaO	Na_2O	K_2O	TiO_2	P_2O_5	LOI	Total
A02	46.37	22.88	9.21	0.04	1.27	0.87	0.56	1.05	1.26	0.08	16.5	100.0
A50	60.66	17.04	5.88	0.09	0.75	0.77	0.94	3.18	1.34	0.06	9.45	100.1

Note: LOI: loss on ignition.

Table 2. Equilibrium pH, cation exchange capacities (CEC), and exchangeable cations of the clay fraction on a sandy fraction <50 µm (A50) and clayey fraction< 2 µm (A02).

Samples	pH±0.1	CEC (chem) meq/100 g ± 5	CEC (UV) meq/100 g ±5	Na^+ (meq/100 g)± 2	K^+ (meq/100 g)± 1	Ca^{2+} (meq/100 g)± 2	Mg^{2+} (meq/100 g) ± 1
A02	9.2	58	62	14.8	1.5	29.2	13.0
A50	9.5	31	34	6.3	0.6	15.8	6.3

Note: Chem: derived from chemical analysis of displaced cations. UV: derived from the measurement of cobaltihexamine concentrations by UV-visible spectroscopy.

shaped aggregates of smectite particles (Figure 3b). TEM-EDX analysis confirms the presence of kaolinite and smectite; and also reveals the additional presence of quartz, feldspar and iron oxy-hydroxides as minor phases (Figure 3c) (Adjia et al., 2013).

Chemical analyses

The major element composition of the alluvial clay fraction is presented in the Table 1 below. The main oxides of alluvial clay fraction <50 µm are SiO_2, Al_2O_3 and Fe_2O_3. The high amount of SiO_2 in the alluvial clay fraction<50 µm is related to its high content in quartz as compared to the alluvial clay fraction. Small amount of MnO, MgO, CaO, Na_2O, K_2O, TiO_2 and P_2O_5 are also found in the two samples. This implied that Mg^{2+}, Ca^{2+} and Na^+ are exchangeable cations of the alluvial clays samples (Adjia et al., 2013).

Physico-chemical characteristics of the alluvial clay

The cation exchange capacity (CEC) values measured from variation in concentration of cobatihexamine match those deduced from the chemical analysis of exchangeable cation for all the samples described herein. This confirms the absence of soluble phases in the studied fraction. The CEC of the clay fraction (Table 2) lie between the values reported in the literature for smectite, that is, 60 to 150 meq/100 g (Adjia et al., 2014). The lower CEC value for A50 fraction compared to clay fraction correlates with its lower content in clays. Indeed, the CEC ratio between A50 and A02 is 0.54, in good agreement with the 57% of clays in A50. From the analyses of the cations exchanged with cobaltihexamine, it can be concluded that around 2/3 of the layer charge is compensated by divalent cations (Ca^{2+} and Mg^{2+}) (Adjia et al., 2013).

Textural

The adsorption-desorption isotherms on the two samples reported in Figure 4 are typical of clay materials containing smectites (Neaman et al., 2003). Numerical values deduced from the adsorption and desorption isotherm are given in Table 3. The difference in the specific surface areas (SSA) of A02 and A50 fractions can be attributed to their quartz content. In fact, A50 fraction contains a large amount of quartz, and quartz particles present low specific surface areas compared to clays. Indeed, the 0.54 SSA ratio between A50 and A02 samples is also consistent with CEC and clay content of A50 showing that sandy fraction of A50 has no surface area. Microporosity represent about 20% of the total surface area and can be assigned to clay layers organisation as generally observed in the case of swelling clays with divalent exchangeable cations (Adjia et al., 2014).

Influence of pH

It appears from Figure 5 that the kinetics of adsorption kinetics of Pb(II) are all the same pace. The balance is reached in less than 5 min, implying that equilibrium had been reached. The amount of Pb(II) adsorbed increases with pH. The amount adsorbed at equilibrium is of the same order for the two samples. The type of thermally

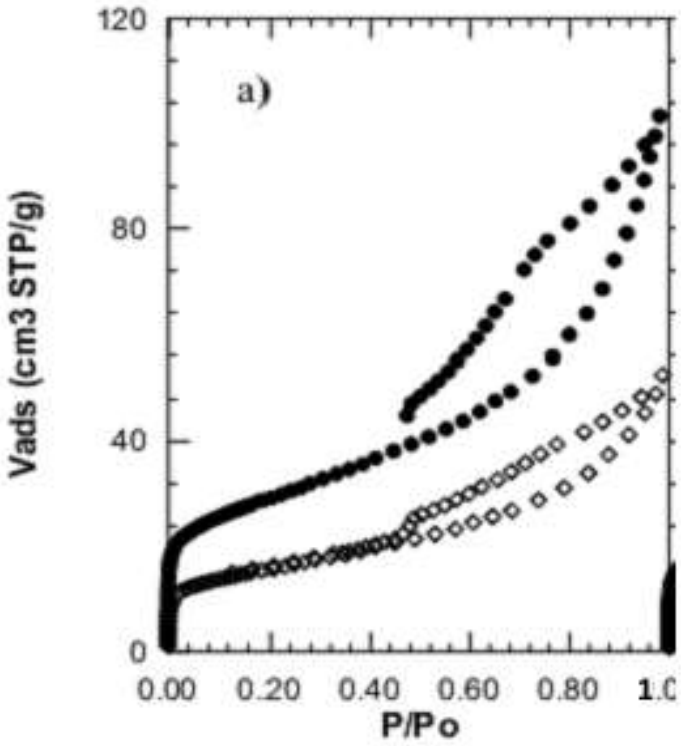

Figure 4. Nitrogen adsorption and desorption isotherms at 77K. For a)clay fraction (A02) and sandy fraction (A50) **●: A02 ; ◊: A50.**

Table 3. Textural parameters deduced from N_2 adsorption desorption isotherms (SSA: specific surface area) on a sandy fraction <50 µm (A50) and clayey fraction< 2 µm (A02).

Samples	BET C constant	BET SSA (m^2/g) ±1	Non Microporous surface area (m^2/g) ± 1	Microporous equivalent surface area (m^2/g) ± 1	Microporous Volume (cm^3/g) ± 0.0003
A02	215	103	82	26	0.0091
A50	337	56	44	15	0.0053

Note: SSA: specific surface a

treatment of alluvial clay and salts solutions do not influence this adsorption. However, as the pH is increased, the removal increases as seen from plots of 2, 4 and 6 which gave removals as high as 92.15 and 100.6 µmol/g to Pb(II) as well as 92.68 and 110.5 µmol/g to Fe(II) respectively (Figures 5 and 6). As shown, the maximum biosorption capacity was reached at pH 6 with 100.6 µmol/g to Pb(II) and 110.5 µmol/g to Fe(II), respectively for lead and iron concentration.

As for Pb(II) and Fe(II) in Figure 6, adsorption equilibrium is rapidly reached (92.15 and 92.68 µmol/g). However, the influence of the pH is less marked, with the adsorption done in the same way with the pH 2, 4 and 4. At pH values higher than 7, Fe(II) precipitation occurred. One notes an increase of the quantities adsorbed by 11% when one passes from the pH 4 until the pH 6.

The alluvial clays are known to possess a negative surface charge in solution. As pH changes, surface charge also changes, and the sorption of charged species is affected (attraction between the positively charged metal ion and the negatively charged clay surface). The effect of pH can be explained in terms of pHzpc (zero point of charge) of the adsorbent. Below this pHzpc, the surface charge of the adsorbent is positive. An increase in pH above pHzpc shows a slight increase in adsorption in which the surface of the adsorbent is negatively charged and the sorbate species are still positively charged. The increasing electrostatic attraction

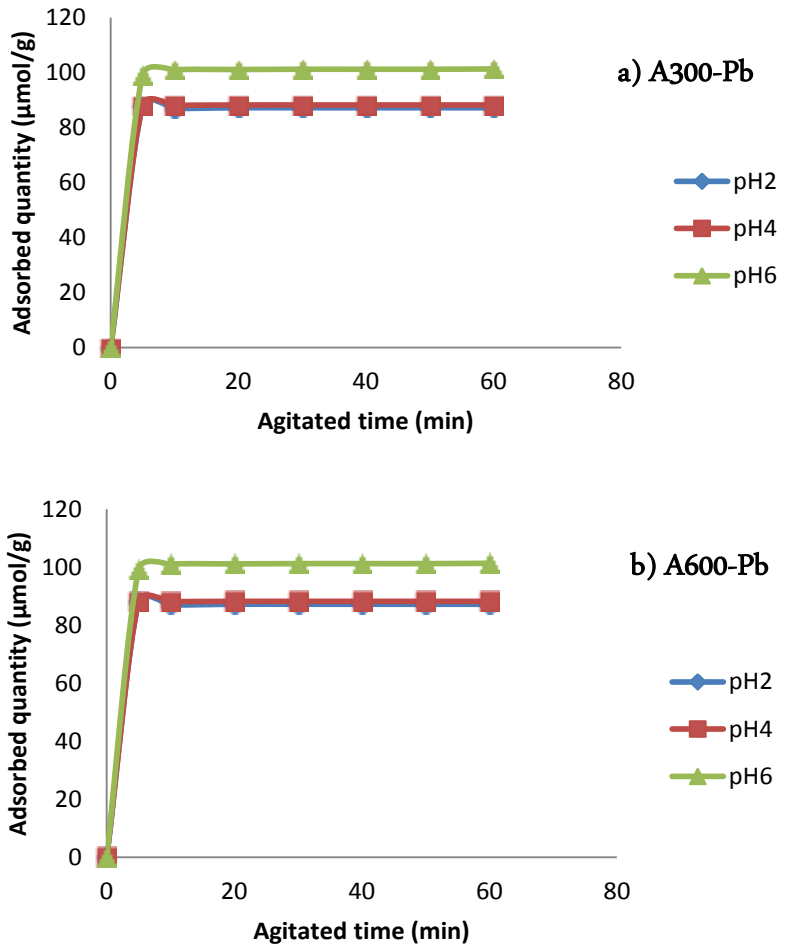

Figure 5. Effect of pH on the kinetics of adsorption of Pb(II) by the treated Alluvial clay thermally at a) 300°C (A300) and b) 600°C (A600): pH=2; pH=4 and pH=6.

between positive sorbate species and adsorbent particles would lead to increased adsorption of metal ions (Kadirvelu et al., 2001).

Influence of temperature

As the temperature is decreased the removal increases as seen from plots of 50, 40 and 30°C which gave removals as high as 99.8 and 100.3 µmol/g to Pb(II) as well as 98.9 and 100.3 µmol/g to Fe(II) respectively. It can be concluded from Figures 7 and 8 that decreasing the temperature increases adsorption. The maximum adsorptions of Pb(II) and Fe(II) ions on thermally treated alluvial clay were found at T= 30°C “to A300 and A600 of Pb(II)” and T= 30°C “to A300 and A600 of Fe(II)”, respectively. Consequently, it is clear that adsorption equilibrium is not a thermo-dependent process, because the alluvial clay is thermally treated. This is mainly because of increased surface activity suggesting that adsorption between metal ion and alluvial clay is an exothermic process (Yasemin and Zübeyde, 2006; Johnson, 1990). Meanwhile, the adsorption capacity was increased as the temperature decreases. So, it should be recognized that the adsorption mechanism is physical.

Modeling the kinetics of adsorption

This helps to investigate the possible mechanisms involved in the adsorption of theoretical Pb(II) and Fe(II) intraparticle diffusion, pseudo-first order and pseudo-second order.

Intraparticular and pseudo-first order diffusion models are not applicable for the explanation of the adsorption of Pb(II) and Fe(II) by our thermally treated alluvial clays at 300 and 600°C given the low values of the R^2 coefficients for these models (Table 4). The coefficients of determination R^2 for the pseudo-second-order kinetic model are close to 1 regardless of the alluvial clay

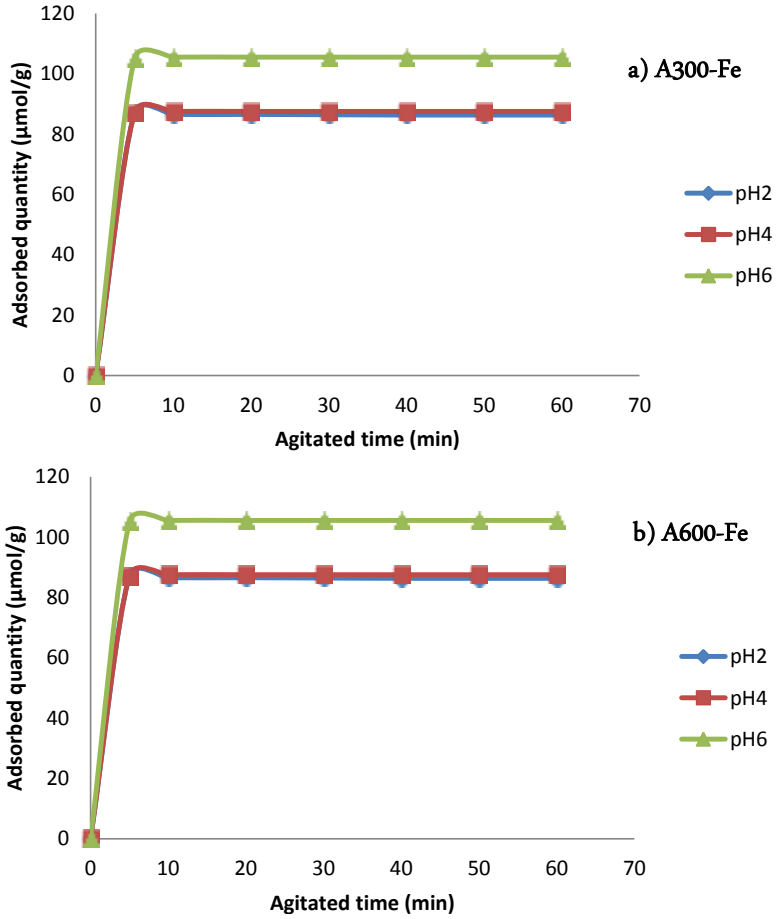

Figure 6. Effect of pH on Fe(II) adsorption kinetics by thermally treated Alluvial clay at a) 300°C (A300) and b) 600°C (A600): pH=2; pH=4 and pH=6.

sample. This shows that the pseudo-second-order kinetic model is particularly suitable for describing the adsorption kinetics of Lead and Iron by our thermally treated alluvial clays at 300 and 600°C.

The first-order kinetic process has been used for reversible reaction with an equilibrium being established between liquid and solid phases (Low et al., 2000). Whereas, the second -order kinetic model assumes that the rate-limiting step may be chemical adsorption (Wu et al., 2001), in many cases, the second-order equation correlates well to the adsorption studies (Sağ and Aktay, 2002). It is more likely to predict that the adsorption behaviour may involve valency forces through sharing of electrons between transition metal cations and adsorbent.

Modeling isothermal adsorption

The Langmuir and Freundlich models are often used to describe equilibrium sorption isotherms. The most widely used Langmuir equation, which is valid for monolayer sorption on to a surface with a finite number of identical sites, is given by Equation 5. The widely used empirical Freundlich equation based on sorption on a heterogeneous surface is given by Equation 6. The calculated results of the Langmuir and Freundlich isotherm constants are given in Table 5. It is found that the adsorptions of Pb(II) and Fe(II) on thermally treated alluvial clay correlated well (R > 0.99) with the Langmuir equation as compared to the Freundlich equation under the concentration range studied. The essential features of a Langmuir isotherm can be expressed in terms of a dimensionless constant separation factor or equilibrium parameter, R_L which is used to predict if an adsorption system is ‘‘favourable’’ or ‘‘unfavourable’’. The separation factor, R_L is defined by:

$$RL = \frac{1}{1+bC0} \quad (8)$$

where C_0 is the initial Pb(II) or Fe(III) concentration (ppm) and b is the Langmuir adsorption equilibrium constant ($ml.mg^{-1}$). Table 6 lists the calculated results. Based on the effect of separation factor on isotherm shape, the R_L

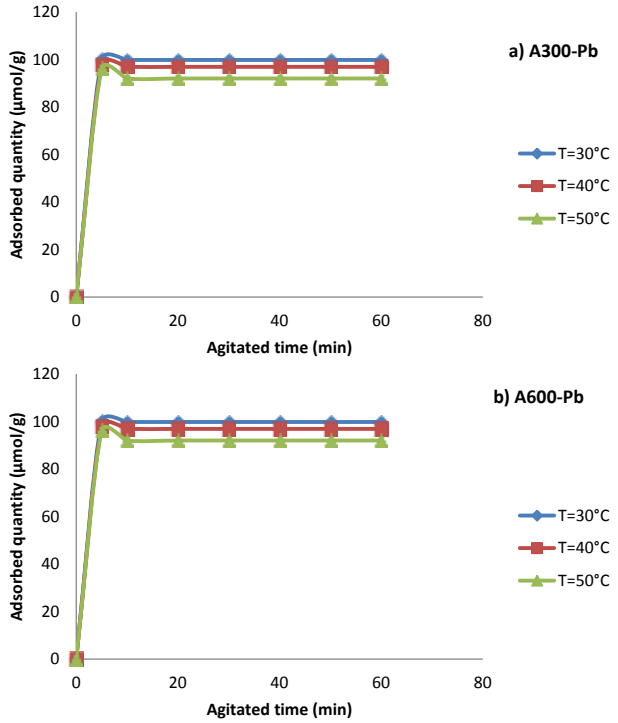

Figure 7. Effect of temperature on the adsorption kinetics of Pb(II) by thermally treated Alluvial clay at a) 300 ° C (A300) and b) 600 ° C (A600): T = 30°C, T = 40°C and T = 50°C.

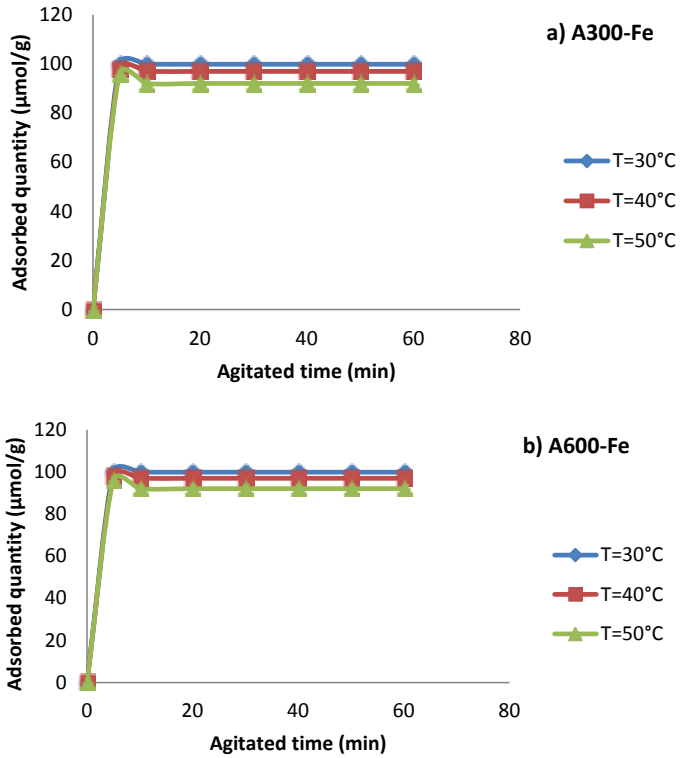

Figure 8. Effect of temperature on Fe(II) adsorption kinetics by thermally treated Alluvial clay at a) 300°C (A300) and b) 600°C (A600): T = 30°C, T = 40°C and T = 50°C.

Table 4. Parameters of kinetic models for the adsorption of lead and iron on thermally treated Alluvial Clay 300°C (A300) and 600°C.

Adsorbents	pH	Lead Pseudo-second order			Iron Pseudo-second order		
		q_{ecal}(µmol/g)	k_2	R^2	q_{ecal}(µmol/g)	k_2	R^2
A300	2	19.92	0.21	0.998	91.74	0.1980	0.999
	4	23.42	0.2145	0.999	93.46	0.1431	0.999
	6	27.55	0.2635	0.999	104.16	0.9216	0.999
A600	2	18.73	0.3752	0.999	91.74	0.0792	0.999
	4	22.32	1.1150	0.999	91.74	0.0848	0.999
	6	26.25	2.0737	0.999	103.09	0.0724	0.999

Table 5. Values of Langmuir and Freundlich isotherms constants.

Pollutants	Adsorbents	Langmuir isotherm			Freundlich isotherm		
		q_m(µmol/g)	b	R^2	n	K_F	R^2
Lead	A300	16.584	-0.063	0.998	1.427	1.062	0.962
	A600	18.620	-0.300	0.982	1.504	1.026	0.981
Iron	A300	94.339	-0.898	0.998	1.054	1.022	0.992
	A600	90.090	-0.572	0.997	1.111	1.016	0.994

values are in the range of $0 < R_L < 1$, which indicates that the adsorptions of Pb(II) and Fe(II) on thermally treated alluvial clay are favourable. Thus, thermally treated alluvial clays are favourable adsorbers. Indeed, the Langmuir model indicates that we have a homogeneous distribution of adsorption sites while the model shows that our adsorbent has a surface heterogeneity.

Conclusion

In this study, enhancing the adsorption of Pb(II) and Fe(II) by the thermally treated alluvial clay from far north Cameroon in the reactor was examined, including equilibrium and kinetic studies. In a view to evaluate their potential use as adsorbent for wastewater treatment, the mineralogical and physico-chemical properties of alluvial clays from far north region of Cameroon has been determined. The alluvial clays reveal that the main mineral present is smectite, kaolinite and quartz. Cation exchange capacity (CEC) and specific surface area of the raw clay fraction are 62 meq/100 g and 104 m^2/g respectively. The main oxides of alluvial clay fraction<50 µm are SiO_2, Al_2O_3 and Fe_2O_3. The overall formula of the clay mineral which was established are: smectite, $[Si_{3.42}Al_{0.58}]_{tetra}[Al_{0.87}Fe_{0.96}Mg_{0.17}]_{octa}\ O_{10}(OH)_2(C^+)_{0.75}$; and kaolinite, $Si_2Al_{1.95}Fe_{0.05}O_5(OH)_4$.

As the pH is increased, the removal increases as seen from plots of 2, 4 and 6 which gave removals as high as 92.15 and 100.6 µmol/g to Pb(II) and 92.68 and 110.5 µmol/g to Fe(II) respectively. As the temperature is decreased the removal increases as seen from plots of 50, 40 and 30°C which gave removals as high as 99.8 and 100.3 µmol/g to Pb(II) and 98.9 and 100.3 µmol/g to Fe(II) respectively. Meanwhile, the adsorption capacity was increased as the temperature decreases. So, it should be recognized that adsorption mechanism is physical. The adsorption process of Pb(II) and Fe(II) are best described by the second-order equation. In our case, the second-order equation correlates well to the adsorption studies. It is more likely to predict that the adsorption behaviour may involve valency forces through sharing of electrons between transition metal cations and adsorbent. However, the adsorption isotherms could be well fitted by the Freundlich equation, which proves the surface heterogeneity of thermally treated alluvial clay. The R_L values are in the range of $0 < R_L < 1$, which indicates that the adsorptions of Pb(II) and Fe(II) on thermally treated alluvial clay are favourable. The clogging is not the problem during adsorption phenomenon in agitated reactor with thermally treated alluvial clay. Finally, the thermally treated alluvial clay, as low cost adsorbent is a favourable adsorber for a growing country.

CONFLICT OF INTERESTS

The authors have not declared any conflict of interests.

ACKNOWLEDGEMENTS

The authors are grateful to all members and teachers of the Applied Chemistry Laboratory ENSAI, Department of Chemistry (FS) for the efforts made towards the success of this work.

REFERENCES

Abdullah A, Moonis AK, Hameed BH, Ayoub AA, Masoom RS, Zeid AA, Yacine B, HadjA (2017). Mercerized mesoporous date pit activated carbon—A novel adsorbent to sequester potentially toxic divalent heavy metals from water. PloS one 12(9):e0184493

Adjia H, Zangué FV, Kamga R (2014). Dépollution des eaux usées par les argiles alluviales. Editions à EUE d'un livre, Référence du livre : 978-613-1-59387-1 (ISBN 978-613-1-59387-1); ISBN-10: 6131593876; EAN: 9786131593871; Maison d'édition: Editions universitaires europeennes; Site Web: http://www.editions-ue.com/; Publié le:18-09-2014.

Adjia H, Zangué FV, Kamga R, Thomas F (2013). Mineralogy and physico-chemical properties of alluvial clays from far-north region of Cameroon: A tool for an environmental problem. International Journal of Water Resources and Environmental Engineering 5(1):54-66, January 2013 Available online at http://www.academicjournals.org/IJWREE DOI: 10.5897/IJWREE12.117 ISSN 1991-637X ©2013 Academic Journals.

Ahmad T, Rafatullah M, Ghazali A, Sulaiman O, Hashim R, Ahmad A (2011). Oil palm biomass based adsorbents for the removal of water pollutants—a review. Journal of Environmental Science and Health, Part C 29:177-222.

Ahmad T, Mohammad D, Mohammad R, Arniza G , Othman S, Rokiah H, Mohamad N, Mohamad I (2018). The use of date palm as a potential adsorbent for wastewater treatment: a review, Environmental Science and Pollution Research 19:1464-1484 DOI 10.1007/s11356-011-0709-8.

Arif TJ , Mudsser A , Kehkashan S , Arif A , Inho C, Qazi M. Rizwanul H (2015). Heavy Metals and Human Health: Mechanistic Insight into Toxicity and Counter Defense System of Antioxidants. International Journal of Molecular Sciences (ijms) 29592-29630. International Journal of Molecular Sciences 16:29592-29630.

Arwidsson Z, Elgh-Dalgren K, von Kronhelm T, Sjöberg R, Allard B, van Hees P (2010) Remediation of heavy metal contaminated soil washing residues with amino polycarboxylic acids. Journal of Hazardous Materials 173:697-704.

Johnson BB (1990). Effect of pH, Temperature and concentration on the adsorption cadmuin on gethite. Environmental Science and Technology 24(1):112-118.

Berthelot Y, Valton E, Auroy A, Trottier B, Robidoux PY (2008). Integration of toxicological and chemical tools to assess the bioavailability of metals and energetic compounds in contaminated soils. Chemosphere 74:166-177.

Bouras O (2003). Thèse de doctorat, Ecole Doctorale Sciences Technologie et Santé, Faculté des Sciences et Techniques, Université de Limoge (2003).

Bridges CC, Zalups RK (2010). Transport of inorganic mercury and methylmercury in target tissues and organs. Journal of Toxicology and Environmental Health, Part B 13(5):385-410.

CACAR (2003): Canadian Contaminants Assessment Report II, Sources, Occurrence, Trends and Pathways in the physical environment, Northern Contaminants program, Minister of Indian Affairs and Northern Development, Minister of Public Works and Government Services Canada P 332.

Cao X, Dermatas D, Xu X, Shen G (2008). Immobilization of lead in shooting range soils by means of cement, quicklime, and phosphate amendments. Environmental Science and Pollution Research 15(2):120-127.

Carneiro MFH; Oliveira SJM; Grotto D, Batista BL, de Oliveira Souza, VC; Barbosa F Jr. (2014). A systemic study of the deposition and metabolism of mercury species in mce after exposure to low levels of Thimerosal (ethylmercury). Environmental Research 134:218-227.

Chang LW (1977) Neurotoxic effects of mercury: A review. Environmental Research 14:329-373.

Chen CW, Chen CF, Dong CD (2012). Distribution and Accumulation of Mercury in Sediments of Kaohsiung River Mouth, Taiwan. APCBEE Procedia 1:153-158.

Chrastný V, Komárek M, Hájek T (2010). Lead contamination of an agricultural soil in the vicinity of a shooting range. Environmental Monitoring and Assessment 162:37-46.

Coetzee PP, Coetzee LL, Puka R, Mubenga S (2003). Charac-terisation of selected South African clays for defluoridation of natural waters. Water SA 29:331-338.

Curren MS, Liang CL, Davis K, Kandola K, Brewster J, Potyrala M, Chan HM (2015). Assessing determinants of maternal blood concentrations for persistent organic pollutants and metals in the eastern and western Canadian Arctic. Science of the Total Environment 527/528:150-158.

Da Costa ACA., Antunes WM, Luna AS, Henriques CA (2003). An evaluation of copper biosorption by a brown seaweed under optimized conditions. Electronic Journal of Biotechnology 6(3):174-184.

De Boer JH, Linsen BG, et Osinga TJ (1996). Studies on pore systems in catalysts. VI. The universal curve. Journal of Catalysis 4:643-648.

Domga R, Harouna M, Tcheka C, Tchatchueng JB, Tsafam A, Domga, Kobbe DN, Dangwang D (2015). Batch Equilibrium, Kinetic and Thermodynamic Studies on Adsorption of Methylene Blue in Aqueous Solution onto Activated Carbon Prepared from *Bos Indicus Gudali* Bones, Chemistry Journal 1(6):172-181.

Geier DA, King PG, Hooker BS, Dorea JG, Kern JK, Sykes LK, Geier, MR (2015).Thimerosal: Clinical,epidemiologic and biochemical studies. Clinica Chimica Acta 444:212-220.

Harouna M, Tcheka C, Abia D, Kobbe DN, Loura BB, Tchatchueng JB (2015). Kinetic, Thermodynamic and Equilibrium Studies on Adsorption of Alumina and Zinc Ions onto Activated Carbon from Hull Seeds of Moringa Oleifera, International Journal of Engineering Research and Science and Technology 4(4):164-172.

International Agency for Research on Cancer (IARC) (1992). Heavy metals in the environmental health: toxicity and carcinogenicity, IARC Scientfic Publications n°118, Lyon 1992.

Ilyin I, Ryaboshapko A, Afinigenova O, Berg T, Hjellbrekke AG, Lee DS (2002). Lead, cadmium and mercury transboundary pollution in 2000. MSC-E/CCC Technical Report 5/2002.

Ilyin I, Rozovskaya O, Travnikov O, Aas W, Hettelingh JP, Reinds GJ (2003). Heavy metals: transboundary pollution of the environment. EMEP Status report, 2(2003):40.

Sundar K, Vidaya R, Amitava M Chandrasekaran N (2010). High Chromium tolerant bacterial strains from palar river basin : Impact of tannery pollution. Research Journal of Environmental and Earth Sciences 2(2):112-117, 2010 ISSN:2041-0492.

Kadirvelu K, Thamaraiselvi K, Namasivayam C (2001). Adsorp-tion of nickel(II) from aqueous solution onto activated carbon prepared from coirpith. Separation and Purification Technology 24:497-505.

Low KS, Lee CK, Liew SC (2000). Sorption of cadmium and lead from aqueous solutions by spent grain. Process Biochemistry 36:59-64.

Basso MC, Cerrella EG, Cukierman AL (2002). Lignocellulosic Materials as Potential Biosorbents of Trace Toxic Metals from Wastewater. Programa de Investigación y Desarrollo de Fuentes Alternativas de Materias Primas y Energía (PINMATE), Departamento de Industrias, Facultad de Ciencias Exactas y Naturales, Universidad de Buenos Aires, Intendente Guiraldes 2620, Ciudad Universitaria, 1428 Buenos Aires, Argentina Industrial & Engineering Chemistry Research 41(15):3580-3585 DOI: 10.1021/ie020023h Publication Date (Web): June 26, 2002 Copyright © 2002 American Chemical Society.

Moon DH, Cheong KH, Kim TS, Khim J, Choi SB, Ok YS, Moon OR (2010). Stabilization of Pb contaminated army firing range soil using calcinated waste oyster shells. Journal of Korean Society of Environmental Engineers 32(2):185-192.

Neaman A, Pelletier M, Villieras F (2003). The effects of exchanged cation, compression, heating and hydration on textural properties of bulk bentonite and its corresponding purified montmorillonite. Applied

Clay Science 22(4):153-168.
Reddy HKD, Ramana DKV, Seshaiah K, Reddy AVR (2010). Biosorption of Ni(II) from aqueous phase by Moringa oleifera bark, a low cost biosorbent. Desalination, pp 8.
Sağ Y, Aktay Y (2002). Kinetic studies on sorption of Cr(VI) and Cu(II) ions by chitin, chitosan and Rhizopus arrhizus. Biochem. Engineering Journal 12:143-153.
Sameeh AM, Reham IM, Amina RA (2016). Removal of heavy metals from aqueous solutions by means of agricultural wastes: assessments based on biological assay and chemical analysis. Journal of Bio Innovation 5(4):480-505, 2016|ISSN 2277-8330 (Electronic).
Vishal KC, Balakrishman P, Deshmukh SK, Vishal IK (2013). Evaluation of adsorption mechanism in clogging of materials used in drip irrigation system. Journal of Agricultural Engineering 50(3):51-56.
Wu FC, Tseng RL, Juang RS (2001). Enhanced abilities of highly swollen chitosan beads for color removal and tyrosinase immobilization. Journal of hazardous materials 81(1-2):167-177.
Yasemin B, Zübeyde B (2006). Removal of Pb(II) from wastewater using wheat bran. www.elsevier.com/locate/jenvman. Journal of Environmental Management 78:107-113.